

Isolation of a (Dinitrogen)Tricopper(I) Complex

Leslie J. Murray,^{*,†} Walter W. Weare,[‡] Jason Shearer,[§] Alyssa D. Mitchell,[†] and Khalil A. Abboud[†]

[†]Department of Chemistry, Center for Catalysis, University of Florida, Gainesville, Florida 32611, United States

[‡]Department of Chemistry, North Carolina State University, Raleigh, North Carolina 27695, United States

[§]Department of Chemistry, University of Nevada, Reno, Reno, Nevada 89557, United States

Supporting Information

ABSTRACT: Reaction of a tris(β -diketimine) cyclophane, H_3L , with benzyl potassium followed by $[Cu(OTf)]_2(C_6H_6)$ affords a tricopper(I) complex containing a bridging dinitrogen ligand. rRaman ($\nu_{N-N} = 1952\text{ cm}^{-1}$) and ^{15}N NMR ($\delta = 303.8\text{ ppm}$) spectroscopy confirm the presence of the dinitrogen ligand. DFT calculations and QTAIM analysis indicate minimal metal-dinitrogen backbonding with only one molecular orbital of significant $N_2(2p\pi^*)$ and $Cu(3d\pi)/Cu(3d\sigma)$ character (13.6% N, 70.9% Cu). $\nabla^2\rho$ values for the Cu– N_2 bond critical points are analogous to those for polar closed-shell/closed-shell interactions.

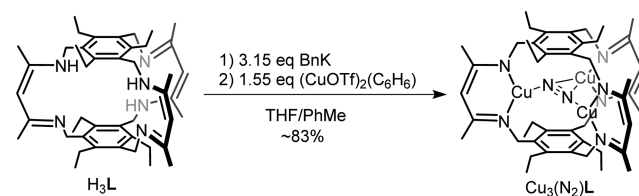
The chemistry of dinitrogen–transition metal complexes has remained an active research focus since the discovery of the pentaamine(dinitrogen)ruthenium(II) complex by Allen and Senoff.¹ Since this seminal work, a number of transition metal–dinitrogen complexes have been reported, which typically feature low-valent low-spin metal centers.² From a survey of all crystallographically characterized compounds, it is immediately apparent however that N_2 adducts of group 11 metals are exceedingly rare, with the N_2 -bridged hexagold cluster as the only reported molecular system.³ For copper(I), computational studies support weak metal-to-ligand π -bonding between the metal and η^2 -alkynes and that the coordination bond is dominated by electrostatics and σ -donation from the alkyne π -bond to metal ion.⁴ Substitution of the ancillary ligands for β -diketiminate (nacnac) or acetylacetonate dramatically enhances the π -backbonding to the bound alkyne; however, copper(I) still remains one of the weakest π -donating metals.⁵ Cu^I-N_2 adducts of the type $X-Cu-N_2$ ($X = Br, F$) have been observed by vibrational or NMR spectroscopy in argon matrix and gas-phase experiments, and a transient $[(bpy)Cu(N_2)]^+$ was generated in electrospray mass spectrometry experiments.⁶ Examples of (dinitrogen)copper(I) species in the solid state are limited to the activated copper-doped zeolites mordenite and ZSM-5 (Cu-ZSM-5) dosed with N_2 .⁷ In particular, dinitrogen binding to the copper centers in Cu-ZSM-5 has been used to probe the nature of the active sites responsible for O atom transfer from either N_xO_y or O_2 to hydrocarbon substrates such as methane.⁸ In all prior reports, a minimal shift was observed for the energy of the N_2 vibration relative to free N_2 , supporting minimal π -backbonding from the cuprous ion(s) to the coordinated dinitrogen as predicted by DFT calculations.⁹

Our general strategy toward studying polynuclear complexes employs the central cavity of polynuclear cyclophane and cryptand complexes as synthetic active sites for the selective binding of small molecule substrates, which subsequently turn-on metal-ion cooperativity.¹⁰ Recently, we reported the synthesis and solution-phase characterization of a tricopper(I) cyclophane complex, which we speculated contained three nominally two-coordinate copper(I) centers.¹¹ Two-coordinate (β -diketiminato)copper(I) complexes are unprecedented and appeared unlikely because of the enforced bent geometry for the copper(I)–ligand interactions. In the absence of a crystal structure, however, we could not construct an alternate model in which a third ligand coordinated to each copper center and yet agree with both the observed three-fold symmetry in NMR spectra and the absence of appreciable halide ions in the elemental analysis results. To our surprise, we report here that this complex contains dinitrogen within the internal cavity of the complex and coordinated to all three copper(I) centers. This compound is the first example of N_2 coordinated to copper(I) centers in a molecular system in either solution or solid state.

Previously, reaction of copper(I) chloride with the potassium salt of a tris(β -diketimine) cyclophane resulted in incorporation of a chloride ligand within the central cavity.¹¹ We previously established that a bromide anion can be accommodated within the internal cavity for the triiron(II) and trimanganese(II) complexes of this ligand.^{10b} $[Cu(OTf)]_2(C_6H_6)$ was used therefore as our metal-ion source to exclude the possibility of any halide donors in the isolated product. Use of this reagent afforded a product that was indistinguishable to the previously reported “ Cu_3L ” by NMR spectra with albeit improved yield (83%, Scheme 1). Slow evaporation of a THF solution of the product complex afforded dark red crystals suitable for single-crystal X-ray diffraction studies.

In the structure of $Cu_3(N_2)L$, each copper(I) center is held within an N,N -chelate of a diketiminate arm, and the metal

Scheme 1



Received: June 26, 2014

Published: September 19, 2014

coordination spheres are completed by the guest N_2 , with disorder for both the copper ions and the dinitrogen ligand (Figure 1). For the copper(I) centers, the primary difference is a

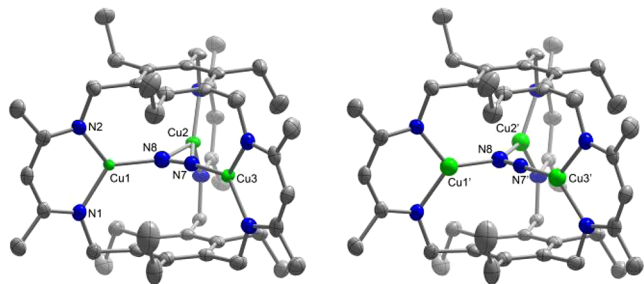


Figure 1. Crystal structure of $Cu_3(N_2)L$ depicting the higher (left) and lower (right) occupancy positions of the Cu^I centers and N7. Occupancy factors for Cu and N atoms sum to 1 and those for Cu1, Cu2, Cu3, and N7 are 0.87, 0.63, 0.75, and 0.75, respectively. C, N, and Cu depicted as gray, blue, and green 80% probability ellipsoids (left) and Cu as spheres (right). H atoms and solvent molecules are omitted.

minor change in the placement of the metal ion relative to the NCCCN plane of the ligand arm to which it is coordinated. In contrast, the disorder in N7 results in two structures in which the N_2 coordination mode is best described $\mu-\eta^1:\eta^2:\eta^1$ (75%, Figure 1, left) and $\mu-\eta^1:\eta^1:\eta^1$ (25%, Figure 1, right). Consequently, the Cu– N_2 bond distances vary slightly with Cu1/Cu1' and Cu3/Cu3' distances between 1.9079(2)–1.8858(1) Å and 1.7772(2)–1.8398(2) Å, respectively. Accounting for the disorder in Cu2, the Cu2/Cu2' and N8 distances vary between 2.2095(2) and 2.0278(2) Å and from 2.0848(2) to 2.7105(2) Å for Cu2/Cu2' and N7. The N–N bond distances are 1.0956(1) and 1.0854(1) Å for the higher and lower occupancy positions of N7, respectively, which are shorter than that for free N_2 and might arise from the observed disorder.¹² Such disorders seem reasonable given that all three ligand arms are equivalent on the NMR time scale and at room temperature. The only other reported clusters containing a $\mu-\eta^1:\eta^2:\eta^1$ -dinitrogen ligand are the cyclopentadienyl trititanium species, and the side-on metal– N_2 bonds are significantly longer for our copper compound, which agrees with less activation of the N_2 ligand by copper(I).¹³ The Cu– N_L (where N_L denotes the ligand N atoms) bond lengths (1.8805(1), 1.9278(2) Å) are significantly shorter relative to all other reported copper(I)-nacnac compounds, but similar to those reported for two-coordinate cuprous ions with two N atom donors.¹⁴

Resonance Raman spectra (excited at 488 nm) were collected on saturated toluene solutions of $Cu_3(N_2)L$ containing either $^{14}N_2$ or $^{15}N_2$ as the atmosphere (Figure 2). We observe a peak at 1952 cm^{-1} in spectra of the $^{14}N_2$ sample, which shifts to 1892 cm^{-1} for a sample degassed and refilled with $^{15}N_2$. The energy for this $\nu(N_2)$ mode is significantly lower than those for $Cu(N_2)$ -ZSM-5 (2295, 2207 cm^{-1}).^{7c,15} The greater extent of π -backbonding for $Cu_3(N_2)L$ as compared to $Cu(N_2)$ -ZSM-5 parallels the stronger π -interactions reported for (β -diketiminato)copper(I) complexes of olefins and alkynes as compared to other ligand systems.^{5d} A very weak absorption is observed in infrared spectrum collected on a solid sample of $Cu_3(N_2)L$ at ~ 1968 cm^{-1} (Figure S1). A similarly weak IR absorption is also observed in a solution sample of $Cu_3(^{15}N_2)L$; however, the expected absorption in the $^{14}N_2$ solution sample is not clearly resolved from other weak vibrations in the sample. Satisfyingly, ^{15}N NMR spectra collected on samples of $Cu_3(^{15}N_2)L$ support

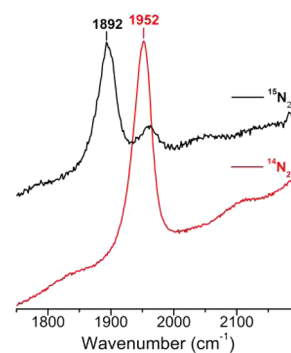


Figure 2. rRaman spectra ($\lambda_{exc} = 488$ nm) of saturated toluene solutions of $Cu_3(N_2)L$ prepared under an $^{14}N_2$ (red) or $^{15}N_2$ (black) atmosphere.

the rRaman and X-ray data with a resonance at 303.8 ppm, which is assigned to $^{15}N_2$ bound within the complex (Figure 3, left). This signal is retained after degassing the sample (Figure 3, right).

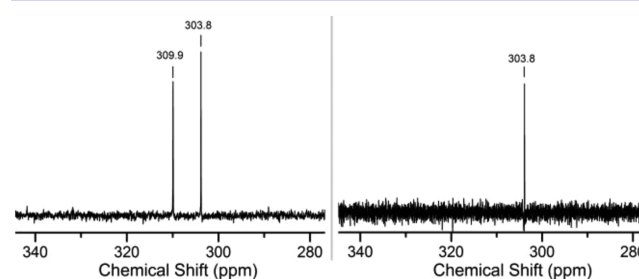


Figure 3. ^{15}N NMR spectra of $Cu_3(^{15}N_2)L$ in d_8 -toluene before (left) and after degassing (right) referenced to $NH_3(l)$. Resonance at 309.9 ppm corresponds to free $^{15}N_2$.

Although examples for which the N–N vibrational frequency is significantly lower than expected for a minimally activated N_2 ligand are reported,¹⁶ the ~ 400 cm^{-1} decrease relative to free N_2 observed here prompted us to perform DFT calculations to probe the metal– N_2 interactions. Geometry optimizations on a truncated model of $Cu_3(N_2)L$ where the Et substituents were replaced with Me groups ($Cu_3(N_2)L^{Me}$) were performed using the BP86 functional (def2-tzvp basis set).^{11,17} The resulting optimized structure agrees with the crystallographic data, and the largest differences are the longer calculated Cu– N_2 (2.231 Å for η^2 , 1.861 Å for η^1) and N–N (1.125 Å) bond lengths. Thus, the calculated structure supports slightly more covalent Cu(I)– N_2 interactions than the crystal structure suggests. Analysis of the formal Cu(3d) orbitals indicates that this bond activation is due to Cu(3d π)/Cu(3d σ) back-bonding into the $N_2(2p\pi^*)$ fragment MO (Figure 4, left). This MO is predominantly Cu(3d) in character, which supports minimal Cu– N_2 bonding; a Löwdin population analysis of this orbital yields an $N_2(2p)$ composition of 13.6% and Cu(3d) composition of 70.9%. This orbital is the only Cu(3d)-based MO with any significant N_2 character.

Two additional computational models were constructed to examine how the ligand alkyl substituents affect the Cu(I)– N_2 interactions. In the first model, Me groups on the phenyl caps were replaced with H atoms ($Cu_3(N_2)L^{PHH}$), and in the second, both the phenyl and nacnac Me groups were substituted with H atoms ($Cu_3(N_2)L^H$). Surprisingly, these minor structural changes lead to differences in the relative position of the nacnac arms, which significantly influences N_2 activation (Figure S2). These ligand distortions translate into a greater degree of N_2

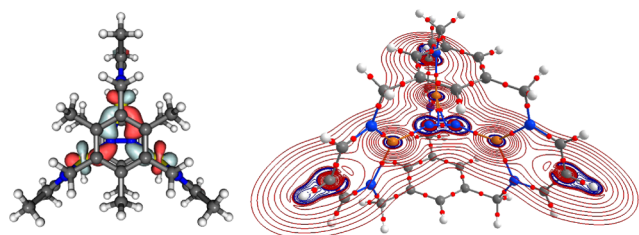


Figure 4. Top-down view of MO-192 (left) and the molecular graph following the QTAIM analysis with bond-paths, bcps (red spheres), and contour plot of $\nabla^2\rho$ in the Cu_3N_2 plane (right) for $\text{Cu}_3(\text{N}_2)\text{L}^{\text{Me}}$. MO-192 is 13.6% $\text{N}_2(2p)$ and 70.9% $\text{Cu}(3d)$. $\nabla^2\rho = -2.7392$ au at the N_2 bcp, which is slightly lower than that for free N_2 .

bond activation relative to $\text{Cu}_3(\text{N}_2)\text{L}^{\text{Me}}$ as indicated by the longer N–N bond lengths (1.167 Å for $\text{Cu}_3(\text{N}_2)\text{L}^{\text{PhH}}$, 1.168 Å for $\text{Cu}_3(\text{N}_2)\text{L}^{\text{H}}$). Expectedly, the calculated N_2 stretching frequencies decrease across this series from 2094.3 cm^{-1} ($\text{Cu}_3(\text{N}_2)\text{L}^{\text{Me}}$), to 1951.5 cm^{-1} ($\text{Cu}_3(\text{N}_2)\text{L}^{\text{PhH}}$), and finally to 1937.2 cm^{-1} ($\text{Cu}_3(\text{N}_2)\text{L}^{\text{H}}$). Similar distortions are observed in the structures of $\text{Fe}_3\text{Br}_3\text{L}$ and $\text{Mn}_3\text{Br}_3\text{L}$, which suggest that these conformations may be accessible in solution.^{10b} We speculate either that the DFT calculations may overestimate the energetic cost of these ligand distortions as compared to the metal– N_2 interactions or that a small energy difference exists between the different ligand conformations. With respect to the molecular structure, crystal packing effects may dominate as suggested by the orientation of two of the Et substituents; 1,3,5-substituted-2,4,6-triethylbenzene derivatives preferentially adopt alternating up–down configurations of the six substituents.¹⁷ However, a number of crystal structures are reported, as for $\text{Cu}_3(\text{N}_2)\text{L}$, in which this conformation is not observed. Subtle effects may then dictate the extent of N_2 activation, and the solution structure likely adopts more activated configuration(s) than the solid-state one.

The extent of N_2 activation in these three model systems was determined using a quantum theory of atoms in molecules (QTAIM) analysis.^{18,19} To obtain an accurate wave function for the QTAIM analysis, we utilized the Sapporo segmented Gaussian all electron basis set. This necessitated the use of a truncated optimization of only the H atoms.¹⁸ The QTAIM analysis supports minimal bond activation for $\text{Cu}_3(\text{N}_2)\text{L}^{\text{Me}}$ with $\nabla^2\rho = -2.7392$ au at the N_2 bond critical point (bcp; Figure 4). This value is more comparable to that calculated for N_2 (–2.9674 au) than N_2H_2 (–1.4642 au) at the same level of theory. Consistent with the geometry optimization and frequency calculations above, the values of $\nabla^2\rho$ at the N_2 bcps are significantly reduced for $\text{Cu}_3(\text{N}_2)\text{L}^{\text{PhH}}$ (–2.1744 au) and $\text{Cu}_3(\text{N}_2)\text{L}^{\text{H}}$ (–1.8009 au) as compared to $\text{Cu}_3(\text{N}_2)\text{L}^{\text{Me}}$ and reflect the greater activation of the N–N bond. Despite these calculated differences for $\nabla^2\rho$ at the N_2 bcps, the values of $\nabla^2\rho$ were ~ 0.3 and ~ 0.5 at the $\text{Cu}-(\eta^1\text{-N}_2)$ and $\text{Cu}-(\eta^2\text{-N}_2)$ bcps, respectively, for all three models and are indicative of closed-shell/closed-shell interactions. We also computationally probed the role, if any, of dinitrogen–benzene interactions on the bond activation and vibrational frequency of the N_2 ligand using the benzene– N_2 –benzene sandwich fragment from the complex. Restraining the phenyl rings at the distance found in $\text{Cu}_3(\text{N}_2)\text{L}^{\text{Me}}$, the N_2 molecule was minimized at the mPW2PLYP/def2-tzvp level. This double-hybrid functional was chosen as it yields more accurate results for weak interactions than pure and hybrid density functional with the empirical dispersive correction. The π – N_2 interactions result in a minimal perturbation to the N_2 molecule relative to free N_2 as evidenced by the bond length

(1.104 Å), vibrational energy (2321.7 cm^{-1}), and $\nabla^2\rho$ value (–2.9335 au) at the N–N bcp, which agrees with previous reports.²⁰

The apparent activation of the N_2 ligand based on the rRaman data versus the fluxionality observed in NMR spectra raises concerns over the extent of covalency between the metal centers and N_2 . Comparison of our data to that for nickel–dinitrogen compounds provides some insight. For the $\text{Ni}^{\text{II}}\text{-N}_2$ species, short N–N bond distances are observed, which correlate with stretching frequencies (2281–2156 cm^{-1}) that are moderately shifted from free N_2 and consistent with predominantly σ -interactions and minimal π -back-donation.²¹ The short $\text{Cu}-(\eta^1\text{-N})$ distances for Cu1 and Cu3 are similar to those for these nickel–dinitrogen adducts with those for Cu1 being analogous to those for nickel(II) (1.905(2) and 1.891(2) Å).^{21b} In contrast, the $\text{Cu}-\text{N}_2$ distances for Cu3 are significantly shorter and similar to those for more reduced nickel compounds, possibly suggesting greater covalency.²² Weak interactions are also reported for mono- and dinuclear nickel(I) and nickel(0) complexes as indicated by N–N bond lengths and the stretching frequency for these compounds. Particularly poignant is the comparison of the series of related nacnac ligated μ -1,2-dinitrogen dimetallic complexes (Table S1).²³ From the observed trend of Fe^{I} to Ni^{I} , the N–N bond distance and vibrational frequency for $\text{Cu}_3(\text{N}_2)\text{L}$ are anticipated to demonstrate no N_2 activation, which is contrary to our result. In the zerovalent series, however, the coordination of the alkali cation(s) to the N_2 donor aids charge transfer from the metals to dinitrogen.^{23c,24} For the dinickel(I) compound, reduction results in a large decrease in the vibrational energy (299 cm^{-1} for the dinickel(I/0) and 428 cm^{-1} for the dinickel(0) species), although the N–N bond distance increases by <0.1 Å for the two-electron reduction. The third copper(I) center in $\text{Cu}_3(\text{N}_2)\text{L}$ may function similarly to the alkali cation(s), leading to the relatively low N–N stretching frequency while not facilitating the extent of charge transfer observed in the zerovalent compounds. Finally, the N_2 binding modes in $\text{Cu}_3(\text{N}_2)\text{L}$ are reminiscent of the calculated intermediates for dinitrogen reduction by an iron(I) diketiminate complex.²⁵ The structure of the tricopper(I)– N_2 adduct provides support for a (μ - η^1 : η^2 : η^1 -dinitrogen)triiron(I) cluster as a plausible early intermediate during N_2 reduction.

In conclusion, $\text{Cu}_3(\text{N}_2)\text{L}$ represents a unique example of N_2 coordinated to copper(I) and provides the first insight into avenues toward designing discrete copper complexes for the selective binding and activation of dinitrogen.

■ ASSOCIATED CONTENT

📄 Supporting Information

Experimental methods, DFT optimized atom coordinates, X-ray crystallographic data in CIF format. This material is available free of charge via the Internet at <http://pubs.acs.org>.

■ AUTHOR INFORMATION

Corresponding Author

murray@chem.ufl.edu

Notes

The authors declare no competing financial interest.

■ ACKNOWLEDGMENTS

L.J.M.: University of Florida and ACS Petroleum Research Fund (ACS-PRF 52704-DNI3), a departmental instrumentation award from the NSF (CHE-1048604), and Prof. A. Roitberg

for assistance with DFT; HT. K.A.A.: NSF (CHE-0821346) and UF for funding X-ray equipment purchase. W.W.W.: Dr. Evgeny Danilov of the NCSU LISF for technical assistance and NC State startup funds. J.S.: NSF CHE-1362662.

REFERENCES

- (1) Allen, A. D.; Senoff, C. V. *Chem. Commun. London* **1965**, 621.
- (2) (a) MacKay, B. A.; Fryzuk, M. D. *Chem. Rev.* **2004**, *104*, 385. (b) Crossland, J. L.; Tyler, D. R. *Coord. Chem. Rev.* **2010**, *254*, 1883.
- (3) Shan, H.; Yang, Y.; James, A. J.; Sharp, P. R. *Science* **1997**, *275*, 1460.
- (4) Nechaev, M. S.; Rayón, V. M.; Frenking, G. J. *Phys. Chem. A* **2004**, *108*, 3134.
- (5) (a) Badiei, Y. M.; Warren, T. H. *Carbene Chem.* **2005**, *690*, 5989. (b) Thompson, J. S.; Bradley, A. Z.; Park, K.-H.; Dobbs, K. D.; Marshall, W. *Organometallics* **2006**, *25*, 2712. (c) Srebro, M.; Mitoraj, M. *Organometallics* **2009**, *28*, 3650. (d) Oguadinma, P. O.; Schaper, F. *Organometallics* **2011**, *28*, 6721.
- (6) (a) Plitt, H. S.; Schnöckel, H.; Bär, M.; Ahlrichs, R. *Z. Anorg. Allg. Chem.* **1992**, *607*, 45. (b) Gatlin, C. L.; Tureček, F.; Vaisar, T. *J. Mass Spectrom.* **1995**, *30*, 775. (c) Francis, S. G.; Matthews, S. L.; Poleshchuk, O. K.; Walker, N. R.; Legon, A. C. *Angew. Chem., Int. Ed.* **2006**, *45*, 6341.
- (7) (a) Kuroda, Y.; Konno, S.-I.; Morimoto, K.; Yoshikawa, Y. *J. Chem. Soc. Chem. Commun.* **1993**, 18. (b) Kuroda, Y.; Yoshikawa, Y.; Konno, S.; Hamano, H.; Maeda, H.; Kumashiro, R.; Nagao, M. *J. Phys. Chem.* **1995**, *99*, 10621. (c) Spoto, G.; Bordiga, S.; Ricchiardi, G.; Scarano, D.; Zecchina, A.; Geobaldo, F. *J. Chem. Soc. Faraday Trans.* **1995**, *91*, 3285. (d) Kuroda, Y.; Yoshikawa, Y.; Emura, S.; Kumashiro, R.; Nagao, M. *J. Phys. Chem. B* **1999**, *103*, 2155.
- (8) (a) Gruenert, W.; Hayes, N. W.; Joyner, R. W.; Shpiro, E. S.; Siddiqui, M. R. H.; Baeva, G. N. *J. Phys. Chem.* **1994**, *98*, 10832. (b) Woertink, J. S.; Smeets, P. J.; Groothaert, M. H.; Vance, M. A.; Sels, B. F.; Schoonheydt, R. A.; Solomon, E. I. *Proc. Natl. Acad. Sci. U. S. A.* **2009**, *106*, 18908. (c) Smeets, P. J.; Hadt, R. G.; Woertink, J. S.; Vanelderden, P.; Schoonheydt, R. A.; Sels, B. F.; Solomon, E. I. *J. Am. Chem. Soc.* **2010**, *132*, 14736. (d) Tsai, M.-L.; Hadt, R. G.; Vanelderden, P.; Sels, B. F.; Schoonheydt, R. A.; Solomon, E. I. *J. Am. Chem. Soc.* **2014**, *136*, 3522.
- (9) (a) Morpurgo, S.; Moretti, G.; Bossa, M. *Phys. Chem. Chem. Phys.* **2007**, *9*, 417. (b) Kisowska, K.; Berski, S.; Latajka, Z. *J. Comput. Chem.* **2008**, *29*, 2677.
- (10) (a) Guillet, G. L.; Sloane, F. T.; Dumont, M. F.; Abboud, K. A.; Murray, L. J. *Dalton Trans.* **2012**, *41*, 7866. (b) Guillet, G. L.; Sloane, F. T.; Ermert, D. M.; Calkins, M. W.; Peprah, M. K.; Knowles, E. S.; Cizmar, E.; Abboud, K. A.; Meisel, M. W.; Murray, L. J. *Chem. Commun.* **2013**, *49*, 6635.
- (11) Di Francesco, G. N.; Gaillard, A.; Ghiviriga, I.; Abboud, K. A.; Murray, L. J. *Inorg. Chem.* **2014**, *53*, 4647.
- (12) In *Crystal Structure Refinement*; Müller, P., Ed.; Oxford University Press, Oxford, 2006; pp 151–152.
- (13) (a) Pez, G. P.; Apgar, P.; Crissey, R. K. *J. Am. Chem. Soc.* **1982**, *104*, 482. (b) Semproni, S. P.; Milsmann, C.; Chirik, P. J. *Organometallics* **2012**, *31*, 3672.
- (14) Selected examples: (a) Khajehnouri, F.; Amstutz, N.; Lucken, E. A. C.; Bernardinelli, G. *Inorg. Chim. Acta* **1998**, *271*, 231. (b) Risto, M.; Takaluoma, T. T.; Bajorek, T.; Oilunkaniemi, R.; Laitinen, R. S.; Chivers, T. *Inorg. Chem.* **2009**, *48*, 6271. (c) Wu, X.-Y.; Kuang, X.-F.; Zhao, Z.-G.; Chen, S.-C.; Xie, Y.-M.; Yu, R.-M.; Lu, C.-Z. *Inorg. Chim. Acta* **2010**, *363*, 1236. (d) Son, K.; Pearson, D. M.; Jeon, S.-J.; Waymouth, R. M. *Eur. J. Inorg. Chem.* **2011**, *2011*, 4256. (e) Huang, Y.-G.; Mu, B.; Schoenecker, P. M.; Carson, C. G.; Karra, J. R.; Cai, Y.; Walton, K. S. *Angew. Chem., Int. Ed.* **2011**, *50*, 436.
- (15) (a) Serykh, A. I.; Amiridis, M. D. *Microporous Mesoporous Mater.* **2006**, *94*, 320. (b) Itadani, A.; Sugiyama, H.; Tanaka, M.; Mori, T.; Nagao, M.; Kuroda, Y. *J. Phys. Chem. C* **2007**, *111*, 16701.
- (16) Selected examples: (a) Ghilardi, C. A.; Midollini, S.; Sacconi, L.; Stoppioni, P. *J. Organomet. Chem.* **1981**, *205*, 193. (b) Buys, I. E.; Field, L. D.; Hambley, T. W.; McQueen, A. E. D. *Acta Crystallogr., Sect. C: Cryst. Struct. Commun.* **1993**, *49*, 1056. (c) Laplaza, C. E.; Johnson, M. J. A.; Peters, J. C.; Odum, A. L.; Kim, E.; Cummins, C. C.; George, G. N.; Pickering, I. J. *J. Am. Chem. Soc.* **1996**, *118*, 8623. (d) Wiesler, B. E.; Lehnert, N.; Tuczek, F.; Neuhausen, J.; Tremel, W. *Angew. Chem., Int. Ed.* **1998**, *37*, 815. (e) Mankad, N. P.; Whited, M. T.; Peters, J. C. *Angew. Chem., Int. Ed.* **2007**, *46*, 5768. (f) Lee, Y.; Mankad, N. P.; Peters, J. C. *Nat. Chem.* **2010**, *2*, 558.
- (17) Hennrich, G.; Anslyn, E. V. *Chem.–Eur. J.* **2002**, *8*, 2218.
- (18) See SI for details and references.
- (19) Bader, R. F. W. *Atoms in Molecules: A Quantum Theory*; Oxford University Press: Oxford, 1990.
- (20) Selected examples: (a) Wesolowski, T. A.; Parisel, O.; Ellinger, Y.; Weber, J. *J. Phys. Chem. A* **1997**, *101*, 7818. (b) Lee, S.; Romascan, J.; Felker, P. M.; Pedersen, T. B.; Fernández, B.; Koch, H. *J. Chem. Phys.* **2003**, *118*, 1230. (c) Munusamy, E.; Sedlak, R.; Hobza, P. *ChemPhysChem* **2011**, *12*, 3253.
- (21) (a) Zhu, D.; Thapa, I.; Korobkov, I.; Gambarotta, S.; Budzelaar, P. H. M. *Inorg. Chem.* **2011**, *50*, 9879. (b) Tsay, C.; Peters, J. C. *Chem. Sci.* **2012**, *3*, 1313.
- (22) (a) Jolly, P. W.; Jonas, K.; Krüger, C.; Tsay, Y.-H. *J. Organomet. Chem.* **1971**, *33*, 109. (b) Krüger, C.; Tsay, Y.-H. *Angew. Chem., Int. Ed.* **1973**, *12*, 998. (c) Jonas, K.; Brauer, D. J.; Krüger, C.; Roberts, P. J.; Tsay, Y.-H. *J. Am. Chem. Soc.* **1976**, *98*, 74. (d) Waterman, R.; Hillhouse, G. L. *Can. J. Chem.* **2005**, *83*, 328. (e) Pfirrmann, S.; Limberg, C.; Herwig, C.; Stöber, R.; Ziemer, B. *Angew. Chem., Int. Ed.* **2009**, *48*, 3357. (f) Zhu, D.; Thapa, I.; Korobkov, I.; Gambarotta, S.; Budzelaar, P. H. M. *Inorg. Chem.* **2011**, *50*, 9879. (g) Tsay, C.; Peters, J. C. *Chem. Sci.* **2012**, *3*, 1313. (h) Harman, W. H.; Lin, T.-P.; Peters, J. C. *Angew. Chem., Int. Ed.* **2014**, *53*, 1081. (i) Kim, Y.-E.; Kim, J.; Lee, Y. *Chem. Commun.* **2014**.
- (23) (a) Smith, J. M.; Lachicotte, R. J.; Pittard, K. A.; Cundari, T. R.; Lukat-Rodgers, G.; Rodgers, K. R.; Holland, P. L. *J. Am. Chem. Soc.* **2001**, *123*, 9222. (b) Ding, K.; Pierpont, A. W.; Brennessel, W. W.; Lukat-Rodgers, G.; Rodgers, K. R.; Cundari, T. R.; Bill, E.; Holland, P. L. *J. Am. Chem. Soc.* **2009**, *131*, 9471. (c) Pfirrmann, S.; Limberg, C.; Herwig, C.; Stösser, R.; Ziemer, B. *Angew. Chem., Int. Ed.* **2009**, *48*, 3357.
- (24) (a) Smith, J. M.; Sadique, A. R.; Cundari, T. R.; Rodgers, K. R.; Lukat-Rodgers, G.; Lachicotte, R. J.; Flaschenriem, C. J.; Vela, J.; Holland, P. L. *J. Am. Chem. Soc.* **2006**, *128*, 756. (b) Horn, B.; Pfirrmann, S.; Limberg, C.; Herwig, C.; Braun, B.; Mebs, S.; Metzinger, R. *Z. Anorg. Allg. Chem.* **2011**, *637*, 1169.
- (25) Figg, T. M.; Holland, P. L.; Cundari, T. R. *Inorg. Chem.* **2012**, *51*, 7546.